ResearchGate

See discussions, stats, and author profiles for this publication at: https://www.researchgate.net/publication/251267712

Spray Drying, Spray Pyrolysis and Spray Freeze Drying

Article · December 2011

DOI: 10.1007/978-1-4419-7264-4_37

CITATIONS
11

READS
1,718

2 authors:

Morteza Eslamian
University of Michigan-Shanghai Jiao Tong University Joint Institute- China
136 PUBLICATIONS **2,028** CITATIONS
SEE PROFILE

Nasser Ashgriz
University of Toronto
165 PUBLICATIONS **2,829** CITATIONS
SEE PROFILE

Some of the authors of this publication are also working on these related projects:

Project Nanoparticle research View project

Project Thermodiffusion, thermophoresis in complex mixtures and nanofluids View project

All content following this page was uploaded by Morteza Eslamian on 21 September 2015.

The user has requested enhancement of the downloaded file.

Chapter 37
Spray Drying, Spray Pyrolysis and Spray Freeze Drying

M. Eslamian and N. Ashgriz

Introduction

In conventional spray pyrolysis (CSP or simply SP), a solution is sprayed into a carrier gas forming small droplets; owing to the high temperature of the surrounding gas, the solvent is vaporized and the solute is precipitated on and within the droplets. If the air temperature is high enough, solute is decomposed to form final solid particles. A schematic diagram of the spray pyrolysis process is shown in Fig. 37.1 [1]. Spray drying (SD) is similar to spray pyrolysis, except that there is no chemical decomposition in SD and usually the process temperature is lower. SP and SD techniques may produce fully-filled or hollow particles depending on the operating conditions. In general, for most materials, hollow particles are formed if at the onset of solute precipitation on the droplet surface, the solute concentration at the droplet center is lower than the equilibrium saturation (Jayanthi et al. [2]). However, Chau et al. [3] showed that Jayanthi's model is not applicable to the formation of NaCl particles.

Spray Freeze Drying (SFD) is a method of producing biopharmaceutical powders that are sensitive to high process temperatures, which may be experienced in spray drying (SD). The detail of the process is described by Costantino and Pikal [4]. This method involves the atomization of a precursor solution, such as protein plus a suitable substance that carries the droplets, into liquid nitrogen. The ice is removed from the frozen droplets by sublimation under vacuum. As this process involves no heat for drying, the denaturation associated with the spray drying process can be avoided. Still, aceptic powder handling is needed and the production yields are low.

A variation of this process is spray freezing into liquid, where the impingement of the feed solution onto the cryogenic liquid results in intense atomization into

M. Eslamian (✉) and N. Ashgriz (✉)
Department of Mechanical and Industrial Engineering, University of Toronto, Canada
e-mail: m.eslamian@utoronto.ca; ashgriz@mie.utoronto.ca

N. Ashgriz (ed.), *Handbook of Atomization and Sprays*,
DOI 10.1007/978-1-4419-7264-4_37, © Springer Science+Business Media, LLC 2011

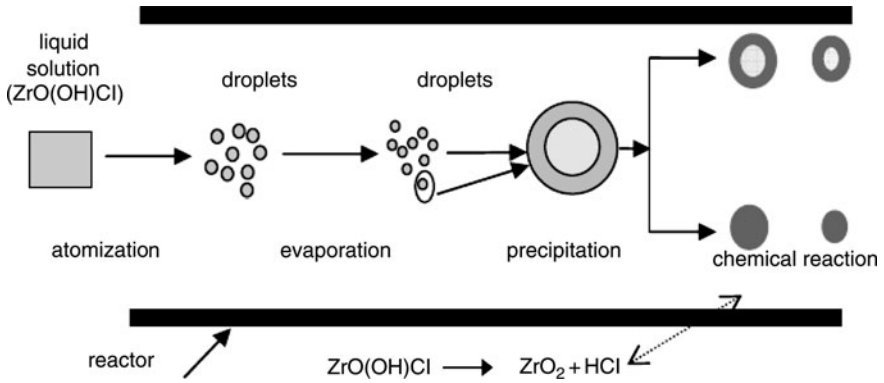

Fig. 37.1 Basic steps of spray pyrolysis method for zirconium hydroxychloride (ZrO(OH)Cl). Once the (ZrO(OH)Cl) powders are relatively dried, they decompose to ZrO_2 and HCl gas. ZrO_2 powders remain in the collector and HCl gas goes to the carrier gas. (Reproduced from [1] with permission. Copyright 2006 Institute of Physics)

micro-droplets, which freeze instantly. The microparticles can then be separated by sieving or evaporation of the cryogen and the sublimation of the solvent. Spray freezing into liquid allows particularly good size control and fast freeze, but it still involves aseptic powder handling.

Recently SFD has attracted the attention of formulation scientists. Spray-freeze drying of aqueous solutions of pure proteins or protein/sugar combinations (Maa et al. [5]) produced larger, more porous particles than those prepared by SD. When the modeling of SFD process is concerned, a mathematical model based on a steady-state heat-transfer condition has been derived by Maa and Prestrelski [6] that can be used to estimate the freezing time in liquid nitrogen, for instance.

Powder Characteristics

Operating conditions, such as the process temperature, ambient pressure and humidity, and also solution characteristics, such as its concentration and type, affect the shape, morphology and structure of the final particles. Effect of various parameters on powder characteristics has been studied both theoretically and experimentally. Several mathematical models for the conversion of solution droplets to particles have been developed, each of which focus on few specific aspects of the process [2, 7, 8]. Following a different approach, Farid [9] modeled drying of single solution droplets focusing on spatial temperature variations within a droplet which is the case for drying of large droplets ($\sim$1 mm), such as milk. Recently, Eslamian et al. [1, 10] modeled evaporation of micron-sized and nano-sized solution droplets and particle evolution and evaporation at various process pressures and temperatures. Their model is applicable to all droplet-to-particle processes, such as SP and SD.

The fundamental equations governing the process [10] are given in Chapter 40, Emulsion Combustion Method, where the basic phenomena involved in evaporation of solution droplets and evolution of particles are described mathematically. It should be noted that, especially for industrial SD process, commercial packages are available to simulate the process but only from a macroscopic point of view. These packages do not consider the detail of the molecular phenomena involved and just provide general information of the overall process.

The most important parameter affecting the morphology of powders is the process temperature. This is because the temperature has a great influence on the solvent evaporation rate. As discussed by Jayanthi et al. [2], for a particular precursor, at given operating conditions, the morphology of particles and whether they are solid and fully-filled, or hollow and disrupted, depends on the concentration distribution within the droplet. The concentration distribution is a strong function of the process temperature.

Figure 37.2 shows the effect of reactor temperature on the solute concentration profile at the onset of precipitation within a droplet with 5 μm initial diameter for a given initial droplet number density, N_0, carrier gas flow rate, Q, and initial relative humidity, RH_0, and initial solution concentration, C_0 [10]. The tubular reactor's inside diameter is 10 mm. The concentration profile inside the droplet depends on the operating conditions and reactor geometry. For reactor conditions of their study

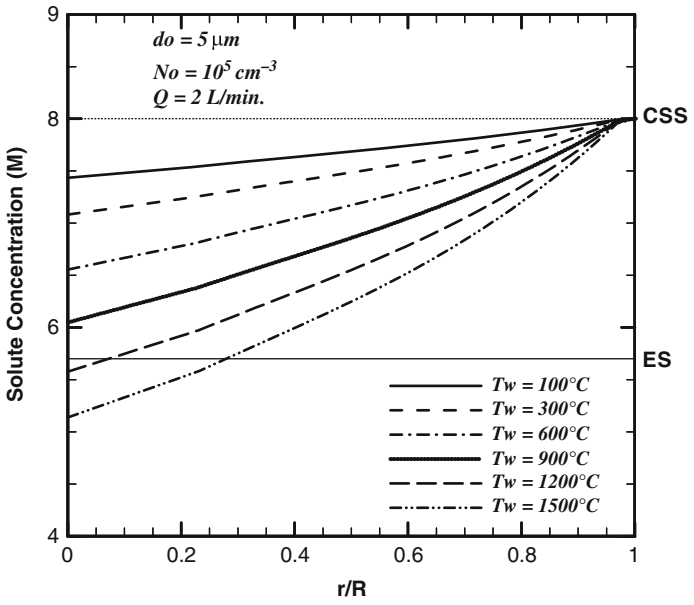

Fig. 37.2 Solute concentration profile within the droplet for various wall temperatures for given initial droplet size d_0, droplet number density N_0, carrier gas flow rate Q, initial relative humidity, $RH_0 = 10\%$, and initial solute concentration $C_0 = 2$ M. (Reprinted from [10] with permission. Copyright 2009 of Taylor & Francis)

as specified above, and for the wall temperatures up to about 1,000°C, the concentration profile entirely lies above the Equilibrium Saturation (ES) line, which is favorable for the production of fully-filled particles [2].

The gradient of the concentration within the droplet depends on the characteristic time of the droplet evaporation and solute diffusion from the droplet surface to the droplet center. As the reactor wall temperature and therefore the reactor bulk temperature increase, the solvent evaporation rate increases, and the characteristic time of evaporation compared to that of solute diffusion decreases. As a result, at high temperatures, at the onset of precipitation on the droplet surface, the concentration in the vicinity of the droplet center falls below the ES line. The occurrence of this type of concentration profile is an indication of having hollow particles as postulated by Jayanthi et al. [2].

Figure 37.3 shows the variations of non-dimensional droplet diameter squared in the shrinkage period as a function of distance from the reactor inlet for various reactor wall temperatures, T_w, for given d_0, N_0, Q, RH_0, and C_0. At reactor wall temperature of 200°C, in order for the shrinkage period (period during which no solute is precipitated yet) to terminate, the droplets need to travel 500 mm from the reactor inlet, whereas for the case of the reactor wall temperature of 1,000°C, this length is reduced to 50 mm. It is observed that the variation of droplet diameter squared with x (and therefore t) is not linear. In fact, it seems that the rate of droplet size reduction ($\sim$ evaporation rate) increases with distance from the reactor inlet.

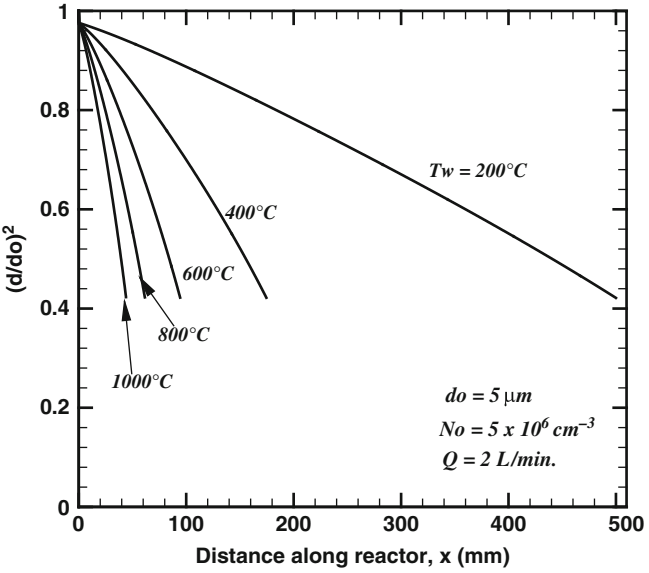

Fig. 37.3 Non-dimensional droplet diameter variations as a function of distance from the reactor inlet for various T_w, for given d_0, N_0, Q, RH_0, and C_0. Reactor inlet gas and droplet temperatures are 25°C $RH_0 = 10\%$, and initial solute concentration $C_0 = 2$ M. (Reprinted from [10] with permission. Copyright 2009 of Taylor & Francis)

One reason is that in spite of the reactor wall temperature, which is constant during the process, the reactor bulk temperature increases with the distance from the reactor inlet. Droplet evaporation rate is a function of the reactor bulk temperature. Also, note that regardless of the reactor wall temperature, the non-dimensional droplet diameter at the onset of precipitation for all cases is almost the same.

Eslamian and Ashgriz [11, 12] systematically investigated the effect of pressure on powder morphology and other powder characteristics. Particle shape and morphology depends on the precursor properties and precipitation mechanism, as well as on the droplet evaporation rate. Droplet evaporation rate is a function of the reactor pressure and temperature. Evaporation rate controls the solute distribution profile within the droplet, and determines whether the particles are solid or hollow. Eslamian and Ashgriz [11] have shown that, when the ambient pressure is reduced to 60 Torr, the decrease of the evaporation rate due to the non-continuum effects is about 60% of that of the continuum-based evaporation rate.

In SP, a low evaporation rate is favorable for the production of less hollow and more fully-filled particles. On the other hand, depending on the nature of the precursor, a relatively high reactor temperature, which causes a high evaporation rate, is essential for a chemical decomposition to occur within the precursor. Hence to increase the likelihood of forming solid particles, it is advantageous to conduct the SP process at reduced pressures.

Figures 37.4 and 37.5 show scanning electron microscope (SEM) images of zirconia powders produced by SP of a 1.0 mol/L solution of zirconium hydroxychloride (ZHC) at two reactor pressures, and at 100°C and 400°C, respectively. A vibrating mesh nebulizer was employed as spray generator. For each reactor ambient pressure, four SEM images at four different magnifications are displayed. At 100°C, particles are spherical and are mostly non-disrupted. The contrast variation in the SEM images shows that depending on the pressure, the particles are either shelly or have smooth surfaces. Figure 37.5 shows that at 400°C, regardless of the pressure, most of the particles are disrupted. The high magnification images show that the particle surface is uneven in this case. The average mean size of the

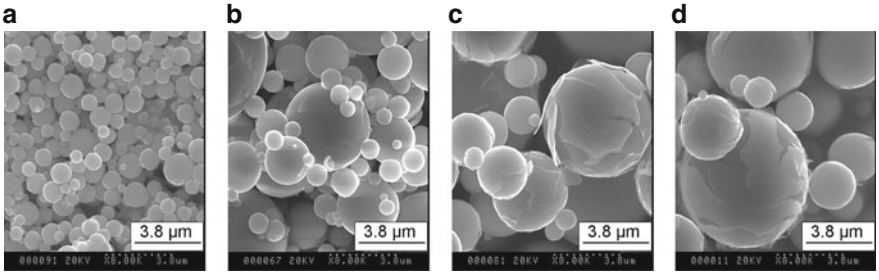

Fig. 37.4 SEM images of zirconia particles produced by spray pyrolysis of a 1.0 mol/L solution of ZHC at 100°C and at, (**a**) 760 Torr, (**b**) 400 Torr, (**c**) 250 Torr, and (**d**) 120 Torr

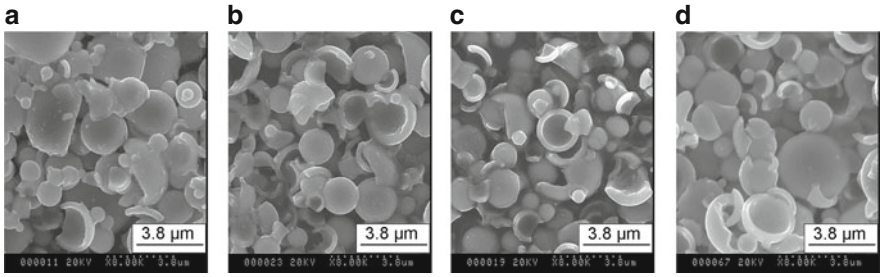

Fig. 37.5 SEM images of zirconia particles produced by spray pyrolysis of a 1.0 mol/L solution of ZHC at 400°C and at (**a**) 760 Torr, (**b**) 400 Torr, (**c**) 250 Torr, and (**d**) 120 Torr

powder at each reactor condition is provided in the figures. In general, as the reactor pressure decreases the size of the particles increases. On the other hand, at low pressures, as the reactor temperature increases, the increasing effect of the pressure on the particle size decreases. Although the pressure variation and, consequently, evaporation rate results in the variation of particle size, other effects, such as the variation of the initial droplet size may also be responsible for the substantial change in the particle size in low pressures. At low pressures, droplet number density and the dispersion behavior of the spray changes. If there is no air to interrupt the droplets, it is expected to see a narrow column consisting of thousands of droplets moving together. This close movement of droplets can result in droplet collision and coalescence. On the other hand, at 760 and 400 Torr the surrounding air disperses the droplets more effectively and the probability of droplet collision and coalescence decreases.

Figures 37.6 and 37.7 show SEM images of sodium chloride powders produced by spray drying of a 2.5 mol/L solution of NaCl at 760, 400, 250, and 120 Torr, and at reactor temperatures of 100°C and 400°C, respectively. In contrast to zirconia particles that were spherical, these powders are cubic. This is attributed to the crystal growth mechanism of sodium chloride, which is different from zirconia powder.

Effects of atomization method and solute concentration on the morphology of spray dried magnesium sulphate ($MgSO_4$) powders were investigated by Eslamian and Ashgriz [13]. They employed three different spray generators including a vibrating mesh nebulizer, a splash plate nozzle and an air mist atomizer. These spray generators produce droplets with a wide range of size and velocity. It was noted that increasing the initial solution concentration resulted in the formation of thicker-walled particles. It was also observed that increasing the initial solute concentration resulted in a reduction in the number of disrupted particles, which was attributed to an increase in the particle wall thickness and strength due to the increase of solute concentration.

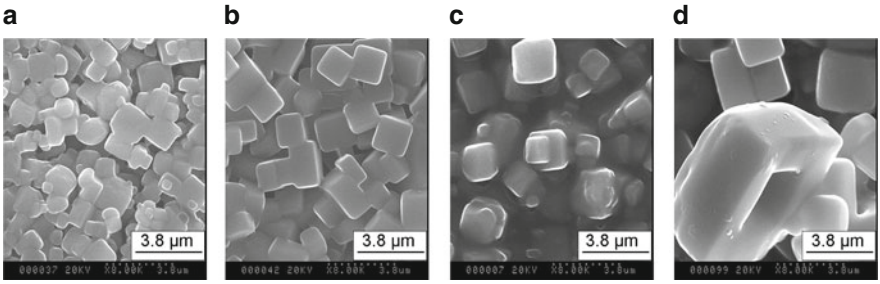

Fig. 37.6 SEM images of the particles produced by spray drying of a 2.5 mol/L solution of NaCl at 100°C and at (**a**) 760 Torr, (**b**) 400 Torr, (**c**) 250 Torr, and (**d**) 120 Torr

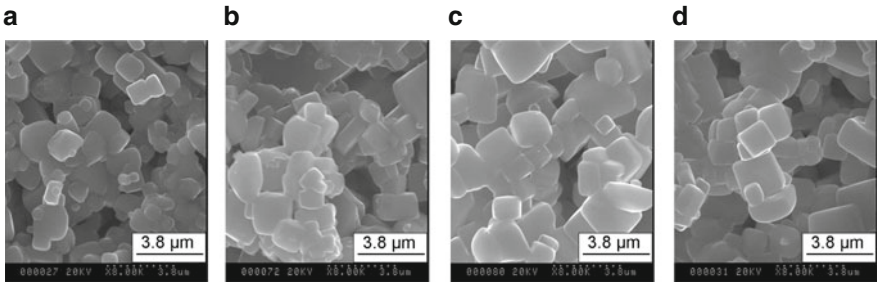

Fig. 37.7 SEM images of the particles produced by spray drying of a 2.5 mol/L solution of NaCl at 400°C and at, (**a**) 760 Torr, (**b**) 400 Torr, (**c**) 250 Torr, and (**d**) 120 Torr

Droplet number density, droplet velocity, presence of atomizing air, and droplet size have substantial effects on particle morphology. Low droplet number density, low droplet velocity and size, and accompanying atomizing air favor rapid droplet drying.

Figure 37.8 summarizes different possible final morphologies for hollow particles formed in SP and SD [13]. If a relative velocity between the air and the droplet exists, a boundary layer will form around the droplet, which results in a non-uniform solvent evaporation and, therefore, a non-uniform crust may form. Depending on the nature of the solute and the process conditions, the crust could be either permeable or impermeable. Pressure buildup in impermeable particles may cause several final particle morphologies. If the crust is uniform and contains no defects, the uniform stress applied on the internal wall of the shell may cause a uniform particle disruption and the particle will be cut into several pieces (type *a*). If the particle wall thickness is not uniform, it may break from the weakest part, and a particle with a small hole may form (type *b*). As another scenario, if the crust is strong enough to resist the internal pressure, the vapor trapped inside the particle

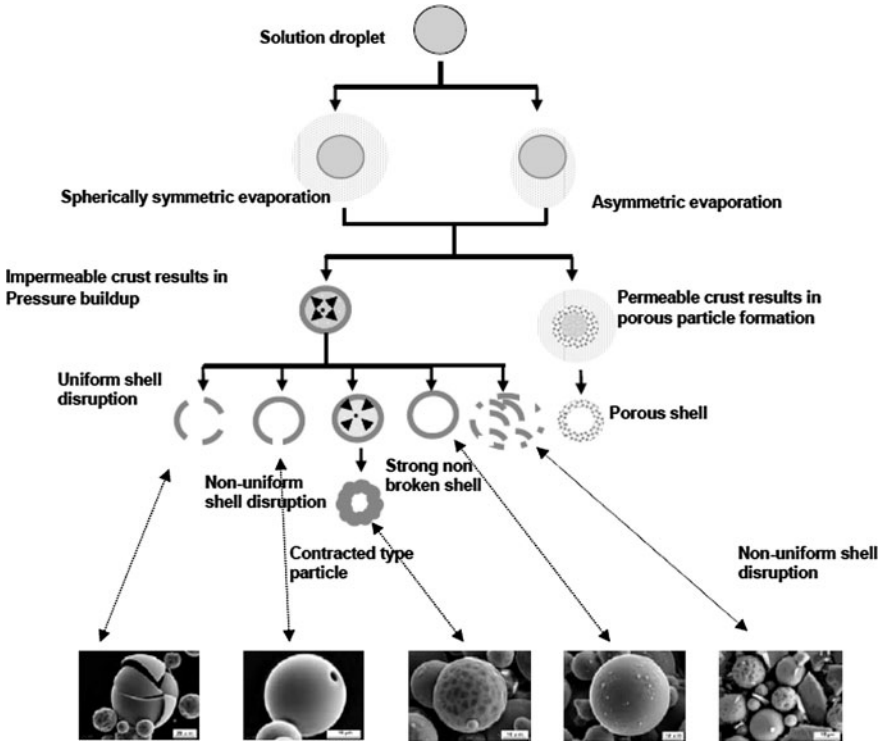

Fig. 37.8 Different possibilities for hollow particle formation during spray drying/pyrolysis. Type (**a**) uniform shell disruption, type (**b**) non-uniform shell disruption, type (**c**) contracted shell particle, type (**d**) non-disrupted smooth surface particle, type (**e**) non-uniform shell disruption, and type (**f**) porous particle. (Reprinted from [13] with permission. Copyright 2007, American Society of Mechanical Engineers)

may later condense and the shell may contract due to depression (type *c*). However, if the shell is fully dried, it is possible that the condensation can not cause any permanent deformation on the particle, and a hollow smooth-surface particle may form (type *d*). In addition, if the crust is thin and weak, or the pressure buildup is substantial, or the particles collide in the reactor, it is possible that the drying particle bursts to form particle flakes (type *e*). On the other hand, for the case of a permeable crust, the evaporated solvent leaves the particle, without increasing the internal pressure, and a non-disrupted porous particle forms (type *f*).

Production of Nanoparticles

As it was stated earlier, typically in SP and SD processes, one droplet in converted into one particle. As a result, the final particle size is dependent on the initial droplet size, unless the particle explodes and fragments into smaller pieces (nanoparticles)

or the solution concentration is very low. In other words, in order to produce nanoparticles via SP and SD processes, one should usually follow one or a combination of the following techniques: (a) use a dilute solution to allow the presence of slight amount of solute in one single droplet, so that finally a nanoparticle forms out of a large droplet; (b) generate nano-sized solution droplets by, for example, electrospraying technique; (c) use a technique to fragment the large mother particle into nanoparticles due to structural breakdown or abrupt solvent evaporation and microexplosion, (d) use a new method called the low-pressure spray pyrolysis. Low-pressure SP is considered in detail in Chapter 38 and the rest are considered below, briefly.

Using a Dilute Solution

This process is conceptually the same as the conventional SP, SD and SFD, except that to guarantee the production of nano-sized particles, the solution concentration has to be very low. A very dilute solution is atomized into small droplets, which may or may not be nano-sized. The solvent, which essentially occupies most of the volume of a solution droplet, evaporates and the remainder of the droplet, i.e., solute produces one nanoparticle. As an example, a salt of the desired semiconductor, such as ZnS, CdS, PbS, and GaN may be dissolved in a solvent to form a solution. Upon solvent evaporation, a stream of unsupported semiconductor nanoparticles are formed and collected on a solid substrate [14].

Electrospraying

In this method, a high voltage is applied to a liquid solution that is flowing through a capillary. Ideally, the liquid reaching the capillary tip forms a Taylor cone, which emits a liquid jet through its apex. When the liquid passes through the spray nozzle, the resulting nanodroplets become charged and produce a droplet stream or a mist due to the repulsive forces between charged particles. During this process, the solvent is vaporized forming charged nanoparticles. These particles then adhere to a substrate having the polarity apposite to that of the particles. By changing the voltage, employing a carrier gas, and placing a plate with a hole between the nozzle tip and the substrate, the migration and deposition of nanoparticles may be controlled to produce desired patterns and nanostructures [15]. This process is schematically shown in Fig. 37.9 [16].

Microexplosion

In the conventional spray techniques, one particle is formed from one droplet. It has been observed that in certain conditions, once a particle is formed, it may somehow

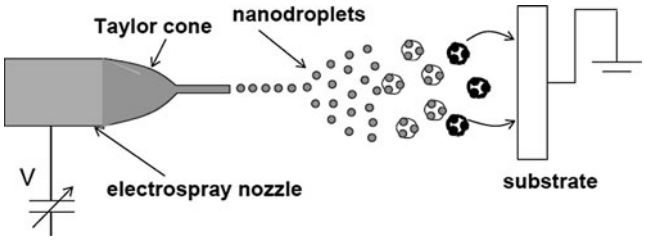

Fig. 37.9 Electrospraying technique for producing nanoparticles by spray methods. (Reprinted from [16] with permission. Copyright 2009 Bentham Science Publishers)

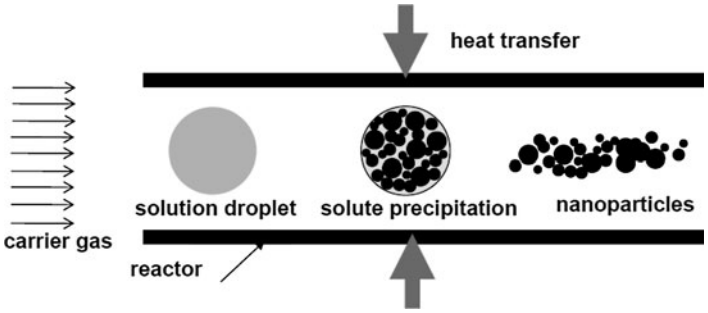

Fig. 37.10 Nanoparticle production method by structural destruction of larger particles. (Reprinted from [16] with permission. Copyright 2009 Bentham Science Publishers)

break down into several smaller pieces including nanoparticles (Fig. 37.10). For instance, in a process called salt-assisted spray pyrolysis, it was observed that provided the droplet/particle temperature exceeds the melting point of the salt added to the main precursor, the salt melts and acts as a high-temperature solvent [17]. The material or its components can then dissolve, undergo reactions, and upon exceeding the solubility limit, precipitate in the solvent. In salt-assisted spray pyrolysis, within a particle, the dissolution/precipitation cycle can lead to the dissolution of some nanocrystallites and the growth of other crystallites by precipitation. This may lead to the breakdown of the particle and disintegration of the individual nanocrystallites. In a process similar to the salt-assisted method, Jakic et al. [18] observed that addition of sodium chloride to the zinc nitrate precursor, even at moderate temperatures, resulted in the disruption of mother particles and the formation of nanoparticles.

Concluding Remarks

In this chapter, fundamentals of spray drying, spray pyrolysis and spray freeze drying processes were described. Using some experimental evidence and modeling results, the effects of operating conditions on characteristics of powders produced

by these methods were reviewed. One of the most important characteristics of a powder is particle morphology and, whether under certain process conditions, particles are hollow or solid and fully-filled. This depends on the condition of the concentration profile developed within the solution droplets, at the onset of solute precipitation on droplet surface. Parameters such as low process temperature, large droplet number density, small initial droplet size, and high initial solution concentration favor the formation of solid fully-filled particles.

In most research studies on SP and SD in the lab scale, ultrasonic atomization has been used to generate droplets/sprays. To increase the powder production rate, other atomization methods should be examined without affecting the particle size, size distribution and quality. For instance, a twin-fluid atomization technique was used to produce lead zirconate titanate (PZT) powder using a starting solution composed of lead acetate, zirconium acetate, and titanium propoxide (stabilized by acetylacetone) dissolved in water by Nimmo et al. [19]. Commercialization of SP technique is closely interrelated to its throughput and strong evidence that SP is a suitable method for the production of some particular advanced powders.

It has been shown that SP is capable of producing composite powders with applications in emerging technologies. In the future, SP will be used to produce a variety of other new composite materials. Fukui et al. [20] synthesized composite powders, such as NiOSDC and La(Sr)CoO_3 by spray pyrolysis, which may be used as anode and cathode of solid oxide fuel cells, respectively. As another example of the application of SP in power production, Bakenov et al. [21] reported the production of stable nano-structured lithium manganese oxide with spherical particles via ultrasonic spray pyrolysis technique. Rechargeable lithium-ion batteries have become the key components for a wide range of portable electronic devices and a promising energy source. The electrochemical performance of the nanostructured $LiMn_2O_4$ prepared was superior to the material prepared by conventional methods.

Another challenge is to address and elucidate the many complex physical and chemical phenomena involved in SP, SD and SFD. In these processes, similar to many other industrial processes, it is important to be able to predict the characteristics of the final product and also to design the components of the equipment and trouble-shoot the operation. Although several attempts have been made to model some aspects of the physical and chemical phenomena involved in these techniques, more work is needed in this area. Currently the commercial packages are adequate in modeling the flow patterns, but are weak when it comes to the intra-particle phenomena. Intra-particle phenomena are more important when the final morphology of particles plays an important role in particle characteristics. Fletcher et al. [22] have addressed the important issues regarding available CFD codes for the industrial spray dryers. They reviewed the fundamental flow behavior in dryers and their modeling using a commercial CFD code. They argued that the key point to emerge is the need to perform three-dimensional, transient calculations and to include hindered drying and wall interaction models. They also noted that coalescence and agglomeration models need to be validated and included in the simulations.

References

1. M. Eslamian, M. Ahmed, and N. Ashgriz: Modeling of nanoparticle formation during spray pyrolysis. *Nanotechnology*, 17, 1674–1685 (2006).
2. G. V. Jayanthi, S. C. Zhang, and G. L. Messing: Modeling of solid particle formation during solution aerosol thermolysis. *Aerosol Science and Technology*, 19, 478–490 (1993).
3. A. Chau, M. Eslamian, and N. Ashgriz: On production of non-disrupted particles by spray pyrolysis. *Particle and Particle Systems Characterization*, 25, 183–191 (2008).
4. H. R. Costantino and M. J. Pikal, Lyophilization of Biopharmaceuticals, Chapter 13: Spray Freeze Drying of Biopharmaceuticals: Applications and Stability Considerations. American Association of Pharmaceuticals Scientists; Springer, Arlington, (2004).
5. Y-F. Maa, P. Nguyen, T. Sweeney, S. Shire, and C. Hsu: Protein inhalation powders: spray drying vs. spray freeze drying. *Pharmaceutical Research*, 16, 249–255 (1999).
6. Y-F. Maa and S. Prestrelski: Biopharmaceutical powders: particle formation and formulation considerations. *Current Pharmaceutical Biotechnology*, 1, 283–302 (2000).
7. Y. Xiong and T. T. Kodas: Droplet evaporation and solute precipitation during spray pyrolysis. *Journal of Aerosol Science*, 24(7), 893–908 (1993).
8. I. W. Lenggoro, I. W. T. T. Hata, F. Iskandar, M. M. Lunden, and K. Okuyama: An experimental and modeling investigation of particle production by spray pyrolysis using a laminar flow aerosol reactor. *Journal of Material Research*, 15(3), 733–743 (2000).
9. M. Farid: A new approach to modeling of single droplet drying. *Chemical Engineering Science*, 58, 2985–2993 (2003).
10. M. Eslamian, M. Ahmed, and N. Ashgriz: Modeling of particle formation via droplet-to-particle spray methods. *Drying Technology*, 27, 1–11 (2009).
11. M. Eslamian and N. Ashgriz: The effect of pressure on the morphology of spray-dried magnesium sulfate powders. *Canadian Journal of Chemical Engineering*, 84(5), 581–589 (2006).
12. M. Eslamian and N. Ashgriz: The effect of pressure on the crystallinity and morphology of powders prepared by spray pyrolysis. *Powder Technology*, 167, 149–159 (2006).
13. M. Eslamian and N. Ashgriz: Effect of atomization method on the morphology of spray generated particles. *ASME Journal of Engineering Materials and Technology*, 129(1), 130–142 (2007).
14. L. Amirav and E. Lifshitz: WO06035425A2 (2006).
15. B. W. Han, J. S. Suh and M. S. Choi: US200693750A1 (2006).
16. M. Eslamian and M. Shekarriz: Recent advances in nanoparticle preparation by spray and microemulsion methods. *Recent Patents on Nanotechnology*, 3(2), 99–115 (2009).
17. B. Xia, I. W. Lenggoro and K. Okuyama: Synthesis of CeO2 nanoparticles by salt-assisted ultrasonic aerosol decomposition. *Journal of Material Chemistry*, 13, 2925–2927 (2001).
18. N. Jakic, J. Gregory, M. Eslamian and N. Ashgriz: Effect of impurities on the characteristics of metal oxides produced by spray pyrolysis. *Journal of Materials Science*, 44(8) 1977–1986 (2009).
19. W. Nimmo, N. J. Ali, R. M. Brydson, C. Calvert, E. Hampartsoumian, D. Hind and S. J. Milne: Formation of lead zirconate titanate powders by spray pyrolysis. Journal of American Ceramic Society, 86(9), 1474–1480 (2003).
20. T. Fukui, S. Ohara, K. Murata, H. Yoshida, K. Miura, T. Inagaki: Performance of intermediate temperature solid oxide fuel cells with La(Sr)Ga(Mg)O-3 electrolyte film. *Journal of Power Sources*, 106(1–2), 171–176 (2002).
21. Z. Bakenov, M. Wakihara and I. Taniguchi: Battery performance of nanostructured lithium manganese oxide synthesized by ultrasonic spray pyrolysis at elevated temperature. *Journal of Solid State Electrochemistry*, 12, 57–62 (2008).
22. D. F. Fletcher, B. Guo, D. J. E. Harvie, T. A. G. Langrish, J. J. Nijdam and J. Williams: What is important in the simulation of spray dryer performance and how do current CFD models perform? *Applied Mathematical Modelling*, 30(11), 1281–1292 (2006).

View publication stats